

Ultra-high Vacuum Technology

The vacuum of the TLS 1.5 GeV electron storage ring has reached an averaged pressure of $< 2 \times 10^{-10}$ Torr (2.6×10^{-8} Pa) at 200 mA beam current after accumulating 6600 Ah beam dose during the past ten years. In 1983, basic study on ultra-high vacuum (UHV) technology was initiated by the former Director of SRRC, Dr. Y. C. Liu, and later a homemade stainless steel (SS) UHV chamber achieved a minimum pressure of 4×10^{-12} Torr in 1985. This is followed by a series of studies focusing on the thermal outgassing rate of the aluminum alloy (AL) chambers led by Dr. J. R. Chen *et al.* In 1987, the experimental measurement of a 3m AL straight chamber resulted in an ultimate thermal outgassing rate of 10^{-14} Torr·L/s·cm² at the lower regime and an ultimate pressure of 7.5×10^{-12} Torr, after vacuum baking. It proved the AL to be an appropriate material for building UHV chamber, even better than SS material, if the water vapor is properly removed from the surface. The techniques of welding the AL vacuum chambers by the tungsten inert gas (TIG) method was developed in Taiwan in 1985, including the setup of humidity controlled clean room for welding and the training of the technicians. A photo of the TIG welding in the humidity- and dust- controlled clean room is shown in Fig. 1. The leakage rate of the TIG welding is kept $< 1.0 \times 10^{-10}$ Torr·L/s as required for all the AL UHV chambers. A homemade surface analyzing UHV system for secondary ion mass spectroscopy (SIMS) was built in 1986 for measuring the impurities in the AL surface oxide layer in the ppm range. It is useful not only for analyzing the surface contamination but also for characterizing the effect of surface cleaning processes, e.g. chemical cleaning, glow discharge cleaning (GDC), etc. A computer program was developed to simulate the pressure distribution of one sextant of the storage ring. These studies finalized the design specifications of the vacuum chambers for the electron storage ring



Fig. 1: TIG welding for an AL bending chamber in the humidity- and dust- controlled clean room.

and the AL was adopted as the base material for the beam ducts. Figure 2 illustrates the data of the measured pressure (dots) in the storage ring during commissioning compared with the simulated result of the pressure distribution (solid curve).

The beam ducts for the storage ring are divided into the straight chambers (S-ch) and the bending chambers (B-ch). The S-ch is made by extrusion method, following by stringent chemical cleaning, and TIG welding to the flanges as well as the pumping chambers. The B-ch is made by the computer-numerical-controlled (CNC) oil-less machining on two AL half pieces in a humidity controlled

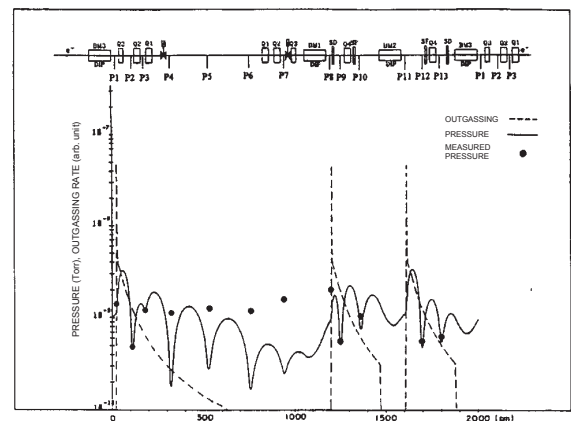


Fig. 2: Comparison between the calculated (solid curve) and measured (dots) results of pressure distribution, at a photon desorption yield of 1×10^{-5} molecule/electron.

house. Figure 3 shows a half piece of B-ch after machining. The received AL pieces shown were immediately sealed in a dry N₂ package after machining to avoid surface contamination during transportation. The TIG welding is applied to join the two half pieces on periphery, after inserting the distributed ion pump (DIP) element. The assembly of one sextant of AL storage ring vacuum system was manufactured and tested. The collaborating local companies not only provide the machining tools in ethanol bath, but also the air-conditioned oil-free clean working environment.

A complete oil-free pumping system is adopted for the storage ring to avoid the backfilled oil contamination. During the earlier commissioning stage, the sorption pumps (SP) and the molecular drag pump (MDP) were used to evacuate the system from atmosphere. The magnetic suspension turbo-molecular pumps (TMP) were switched on at 10⁻² Torr, and operated during the vacuum baking and the commissioning at higher pressure range but limited to < 1 × 10⁻⁶ Torr. The sputtering ionization pumps (SIP) and the St-707 non-evaporable getter (NEG) pumps were not activated before baking nor were operated at the pressure > 1 × 10⁻⁷ Torr, to avoid production of micro-dust or heavy gas load for the absorption materials. A vacuum safety interlock system protects the storage ring from emergency shut down of the TMP and MDP. All the gate valves and the vacuum compo-



Fig. 3: A half piece of the B-ch after oil-free CNC machining.

nents were checked for their function and pre-baked for degassing purpose prior to installation. The result is effective removal of the gas load from the vacuum system and consequently the commissioning period was reduced with very low failure rate.

During the past ten years, large effort has been put on the construction of more than 12 sets of highly reliable compact front end UHV systems, and 14 sets of photon beam position monitors (PBPM) with high resolution of < 0.5 μm. The developments of the UHV technology applied to the upgrade programs include the aluminum beam duct for the insertion devices (ID), the differential pumping systems for the beam lines, the independent absorbers in the storage ring, etc., as will be described in the following sections.

Development the Beam Duct for Insertion Devices

Similar to the long straight section chambers for the electron storage ring, the AL beam ducts for the narrow gap insertion devices (ID), including the undulators, i.e. EPU5.6, U5, U9, and the wigglers, i.e. W20, SWLS, have been developed by the extrusion method. The minimum gap of the ID's is ~ 18 mm for the undulators, and ~ 22 mm for the wigglers. The parameters for the ID chambers are listed in Table 1. A photograph of the beam duct is shown in Fig. 4. A prototype of the AL ID vacuum chamber, 14 mm in outside vertical height and 4 m in total length, has been installed in the storage ring in Feb. 1996 and commissioned for four months paralleling the user beam shifts.

The AL ID beam ducts are made by the extrusion method with slightly thicker upper and lower surfaces. The flatness of the beam duct was controlled to < 0.2 mm for the chambers of 4.5 m in length. Afterwards, both the upper and the lower surfaces proceeded with the CNC machining iterated and slowly to minimize the residual stress yield. The supporting frame with adjusting mechanics, for alignment and positioning, and the sliding joints, for absorption of the thermal expansion during baking, for the ID chamber can only set at one side. The surface machining cannot proceed before the chemical cleaning of the beam

duct following by the TIG welding of the flanges, cooling pipes, and supporting pads. A strip of the NEG pump was installed, along the side of the interior of every ID beam duct except SWLS, to function as a linear pump for evacuating residual gases, out of the electron beam channel, mainly H₂ and CO. The schematic drawing of the NEG strip is shown in Fig. 5. Recently, a spare 4.5 m chamber for U9 ID has been coated the NEG film inside at CERN. This NEG coated chamber is under the exposure testing at the 19B(PSD) beam line at TLS.

Development the Aluminum Differential Pumping System for the Beamlines

Two differential pumping systems were developed as the gas filters for two high flux photon beam lines, 03(HF) and 21B(U9). The purpose is to reduce the intensity of the high order light by 4 orders of magnitude. The pressure of the He gas inside the filter chamber will be 0.5 Torr for 03(HF) and 5 Torr for 21B(U9), while the pressure on both ends of the filter chamber connecting to the beam line should be less than 1×10^{-8} Torr. The gas filter needs to maintain the above pressure difference with a short length of 1.8 m. However, the cross section of gas filter varies from $118 \times 22 \text{ mm}^2$ to $109 \times 42 \text{ mm}^2$ for 03(HF), and from $3 \times 14.94 \text{ mm}^2$ to $3.96 \times 5.18 \text{ mm}^2$ for 21B(U9). The pumping speed is thus limited by constraints of space for the pumps. The aperture of the gas filter cannot be too small since the photon flux transported through the chamber cannot be sacrificed. So the chamber should be designed to fit the shape of the photon beam with a stringent tolerance of ~

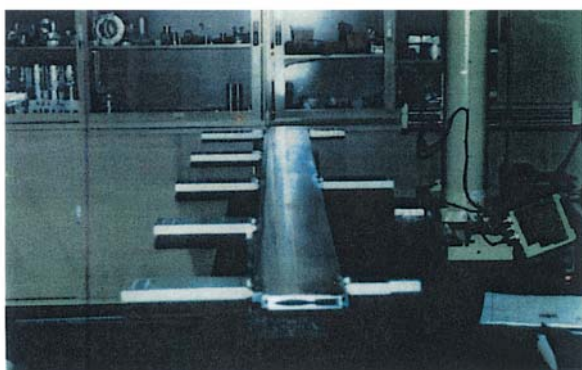


Fig. 4: AL beam duct for the ID.

0.5 mm, and to accommodate five pumping ports for the pumps. In the case of gas filter for 21B(U9), we demonstrated a successful reduction of higher energy photons by a factor of >1000 at 3 Torr of He gas. However, the gas filter for 03(HF) cannot work unless a structure consisting of thin blades, 0.3 mm in thickness, is distributed along the beam axis that divides the inner cross section of gas filter into 22 channels. The conductance of the chamber thus can be reduced by a factor of 22 (~ 5%) through this blade structure that helps the differential pumping efficiency.

The aluminum alloy is adopted as the material of the gas filter chamber for its good machining capability and thermal conductivity. The manufacturing of the gas filter is similar to that of the bending chambers of the storage ring. Figure 6 shows a photograph of the gas filter system. The test result shows a pressure $< 1 \times 10^{-8}$ Torr on UHV side when pressure in the gas cell is 0.1 Torr.

Development of the Independent High Heat Load Absorbers

When the energy of the electron beam increases from 1.3 GeV to 1.5 GeV, the heat load of the synchrotron radiation emitted from the bending magnet is ~ 1.8 times higher. The original design of the bending chamber is to confine the synchrotron radiation to the downstream inner wall of the bending chamber, where the water-cooling channels are drilled inside. However, the temperature of the cooling water can increase ~ 3 °C at the heat load of 200 mA beam current. The thermal expansion of the vacuum chambers due to the change of the heat load pushes the magnet and moves the beam position monitor (BPM) that causes the errors of the beam position readings. In order to reduce the heat load from bending chambers, the independent photon absorbers had been developed, and inserted into the bending chamber through a 150 CF flange such that ~ 50% of the heat load can be removed from the chamber. Three sets of new absorbers have been installed in R1 bending section. A reduction of the temperature rise of the cooling water in the bending chamber from ~ 3 °C to ~ 1.5 °C shows the effectiveness of the new absorbers.

Table 1. Parameters of the beam ducts for the insertion devices.

Section	R1	R2	R3	R5	R6
ID name	SWLS	EPU5.6	U5	W20	U9
λ_u (cm)	20	5.6	5.0	20	9.0
Length (m)	0.8	3.9	3.9	3.1	4.5
Gap (mm)	22	18	18	22.5	18
Inner height (mm)	18	13	13	17	13
Inner width (mm)	100	80	80	80	80
Material	A6063T5 Aluminum Alloy				
Install year	2002	1997	1997	1995	1998

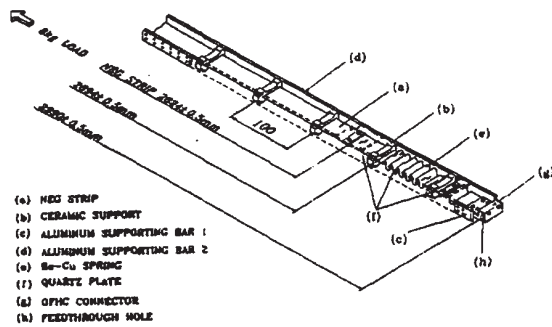


Fig. 5: Schematic drawing of the NEG strip for the ID beam ducts.

A water-cooled copper absorber shown in Fig. 7 was developed and inserted into a ceramic kicker chamber downstream the SWLS in the injection section of the storage ring. Commissioning of SWLS at a field of 5.3 T has been successfully performed. The pressure rise due to the photon stimulated desorption (PSD) has been reduced by the beamself-cleaning. A lifetime of 10 h at beam current of 200 mA was achieved when pressure rise per beam current is 1×10^{-10} Torr/mA at accumulated beam dose of ~ 50 Ah.

Upgrade Planning for the TLS storage ring

We have planned to install three sets of superconducting multipole wigglers (SMPW) in the achromatic bending sections, and one set of superconducting RF cavity (SRF) in the next few years. The electron beam current is expected to be kept at top-up injection mode, and increased from 200 mA to 500 mA. New ceramic kicker chambers and

the bellows will be replaced. The features of the new ceramic chambers include (1) wider horizontal width to protect the brazing part from irradiation; (2) smaller vertical height to reduce the kicker field strength; (3) cooling channel on both sides to remove the heat load input by SWLS photon beam; (4) additional pumping ports on the ceramic chamber to increase the local pumping efficiency.

Some absorbers in the storage ring and front ends will be replaced to accept a higher heat load and to reduce the thermal expansion of the beam chambers. The front ends for the BL12XU and BL12B2 at SPring-8 in Japan have been constructed by SRRRC through collaboration with APCST and SPring-8 faculties. The experiences on the high heat load components and the PBPM will be



Fig. 6: Photograph of the gas filter system for 03(HF).

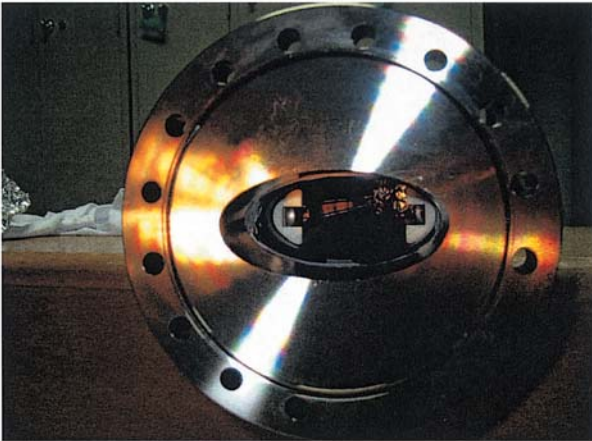


Fig. 7: Photograph of the absorber inside a kicker chamber.

helpful for upgrading the front end systems at NSRRC.

For the cryogenic cold-bore beam duct of SMPW, the molecular desorption yield stimulated by the scattered photons will be measured at the 19B(PSD) beam line. Molecules will be desorbed by the synchrotron irradiation, and soon stick on other surface of the cryogenic beam duct forming a physical absorbed layer. The accumulated molecules frozen on the cryogenic surface will bounce back and forth inside the beam duct when hitting by the scattered light which will produce more desorbed molecules. This phenomenon is called "recycled desorption yield". The recycled and the unstable molecular desorption cause unstable pressure change and bring the system to higher pressure regime. The instability and the lifetime of the electron beam will both become worse. On the other hand, the molecules on both ends of the cryogenic beam duct will migrate from warm chambers into the cold beam duct. It is possible to coat the NEG in the warm chambers near the cold beam duct which functions as an effective linear capture pump.

Author:

G. Y. Hsiung
National Synchrotron Radiation Research Center,
Hsinchu, Taiwan

Publications:

- Y. C. Liu, S. C. Wu, J. R. Chen, and H. S. Tzeng, Chinese J. Phys. **23**, 273 (1985).

- J. R. Chen, K. Narushima, and H. Ishimaru, J. Vac. Sci. and Technol. A **3**, 2188 (1985).
- D. C. Chen, G. Y. Hsiung, and J. R. Chen, J. of Vacuum Society of R.O.C. **1(1)**, 24 (1987).
- J. R. Chen, G. S. Chen, D. J. Wang, G. Y. Hsiung, and Y. C. Liu, Vacuum **41**, 2079 (1990).
- J. R. Chen and Y. C. Liu, Vacuum **44**, 545 (1993).
- G. Y. Hsiung, J. R. Huang, J. G. Shyy, D. J. Wang, J. R. Chen, and Y. C. Liu, J. Vac. Sci. Technol. A **12**, 1639 (1994).
- D. J. Wang, J. R. Chen, G. Y. Hsiung, J. G. Shyy, J. R. Huang, S.N. Hsu, K. M. Hsiao, and Y. C. Liu, J. Vac. Sci. Technol. A **14**, 2624 (1996).
- G. Y. Hsiung, D. J. Wang, J. G. Shyy, S.N. Hsu, K. M. Hsiao, M. C. Lin, and J. R. Chen, J. Vac. Sci. Technol. A **15**, 723 (1997).
- J. R. Chen, T. S. Ueng, G. Y. Hsiung, T. F. Lin, C. T. Lee, S. L. Tsai, and S. L. Chang, J. Synchrotron Rad. **5**, 621 (1998).
- J. C. Lee, T. S. Ueng, J. R. Chen, Y. J. Hsu, G. Y. Hsiung, T. F. Lin, S. H. Chang, S. N. Hsu, D. J. Wang, Nucl. Instr. and Methods in Physics Res. A **467-468**, 793 (2001).

Contact e-mail:

hsiung@nsrrc.org.tw